Modelling masonry structures through the Mady code

2nd International **Conference on Recent Advances in Nonlinear Models** – Design and Rehabilitation of Structures
CoRASS 2017
H. Barros, C. Ferreira, José M. Adam and Norb Delatte (Eds)

MODELLING MASONRY STRUCTURES THROUGH THE MADY CODE

M. LUCCHESI*, B. PINTUCCHI† AND N. ZANI‡

*Department of Civil and Environmental Engineering
University of Florence
via S. Marta 3, 50139 Firenze, Italy
E-mail: massimiliano.lucchesi@unifi.it; webpage: https://www.unifi.it

† Department of Civil and Environmental Engineering
University of Florence
via S. Marta 3, 50139 Firenze
E-mail: barbara.pintucchi@unifi.it, webpage: https://www.unifi.it

‡Department of Civil and Environmental Engineering
University of Florence
via S. Marta 3, 50139 Firenze
E-mail: nicola.zani@unifi.it, webpage: https://www.unifi.it

Key words: masonry structures, finite elements code, numerical tools, models, static analysis, dynamic analysis.
Summary. The paper is aimed at presenting the finite element code MADY and the models formulated on purpose for masonry structures and implemented into the code in the last decade. Beam elements as well as plane, shell and brick elements are available. As for the material models, in the framework of the continuous homogeneous approach, those provided by the code range from the simplest no-tension material to more refined models, accounting for bounded tensile and shear strengths with damage process and plasticity in compression. In the paper, the main features of the code are presented through some static and dynamic analyses of masonry structures, shown for the sake of example.

1 INTRODUCTION

MADY is a non-commercial finite element code for conducting static and dynamic analyses of masonry structures.

Initially developed on the basis of a one-dimensional no-tension model formulated for masonry columns, or masonry slender structures in general[1,2,3,4], the code has been enriched by different and more refined models.

In order to cover different types of masonry structures and capture various and different aspects inherent in the masonry's behavior, the code has been provided by different finite elements – plane, shell and brick isoparametric elements. For what concerns the material's library, a constitutive equation has been formulated for an isotropic elastic material with some constrain imposed by requiring that the stress must belong to a *stress range*, i.e. a non empty,

closed and convex subset of the space of all symmetric tensors of the second order. Masonry-like materials, eventually with bounded compressive strength, belong to this class of hyperelastic materials[5]. In addition, such formulation allows to consider a limited shear stress[6]. For these cases, where the domain of the strength is a polyhedron, the relationship between stress and strain and its derivatives – required to numerically solve the equilibrium and evolution problems[7,8] – have been explicitly evaluated.

The material model allows to account also for an initial bounded tensile strength, that can be progressively decreased according to a prescribed damage law.

Moreover, when dynamic or cyclic loading are applied, the material's behavior may depend on the whole history of deformation; for these cases, a plastic model has also been provided[9].

Lastly, an input/output interface for MADY has been implemented to generate the mesh files and visualize the results.

In the paper, results of static and dynamic analyses for two recurrent masonry typologies– a groin vault and a free-standing bell tower - have been selected to present the main features of the code. For the sake of clarity, idealized structural schemes have been intentionally used.

2 THE MATERIAL MODELS

2.1 Beam models

The development of a *basic* beam element got started from a constitutive equation formulated in terms of generalized stress (normal force and bending moment) as a function of the generalized strain (extensional strain and curvature change of the beams longitudinal axis). This constitutive equation was defined by making the Euler-Bernoulli hypothesis and assuming that the material is unable to withstand tension in the longitudinal direction and has a bounded compressive strength[1,2].

Developed initially for rectangular cross-section, the constitutive relations of the beam have been then formulated for other geometries, such as hollow rectangle, having in mind to model towers or minarets[1,3]. The constitutive model has also been generalized to take into account the presence of a reinforcement, such in case of FRP strengthened arches[9,11].

A bounded shear strength can be accounted for as well as a limited tensile strength. In addition, refined constitutive idealizations to account for adequate post-yield behaviour of masonry in compression and in tension has been defined[9,11]. Specifically, accounting for a linear piecewise law of softening behaviour, the actual stress distribution of a generic cross-section is represented by means of an equivalent section for which the values of the materials Young modulus and compressive strength are updated and reduced through a damage function, if the section is about to evolve into a state with a degree of damage greater than its current state. Obviously, the material thus obtained is no longer elastic, because the damage phenomenon is irreversible.

Over the last ten years, several comparisons of the results obtained through the Mady code with those provided by other models and experimental data have been carried out. Just to cite a few, results of pushover analyses obtained through Mady have been compared with those provided by a considerable number of numerical models, including numerical approaches

specifically developed for masonry buildings (3Muri, 3DMacro, etc.) and general-purpose finite element codes (DIANA, ANSYS and Code ASTER)[3,12]. Results of dynamic analyses have, instead, been compared with those from OpenSees[4] and the NOSA-ITACA code[13].

2.2 Normal elastic and elasto-plastic materials

For plane, shell and brick elements, the constitutive models implemented into the code are the normal elastic and elasto-plastic materials.

For a normal elastic material, the infinitesimal strain tensor E is the sum of two parts, the elastic part E^e from which the stress T depends linearly and isotropically and the anelastic part E^a which belongs to the normal cone $\mathcal{N}_{\mathcal{K}}(T)$ of $\mathcal{K}$ at T. Namely[5]

$$E = E^e + E^a, \quad T = \mathbb{C}E^e, \quad E^a \epsilon \mathcal{N}_{\mathcal{K}}(T), \tag{1}$$

where $\mathbb{C}$ is the tensor of the elastic moduli. Let $\mathcal{E} = \mathbb{C}^{-1}(\mathcal{K})$ be the elastic range. As $\mathcal{E}$ is a closed, non-empty and convex set, for a given strain tensor E, the Minimum Norm Theorem guarantees the existence and uniqueness of the projection $P_{\mathcal{E}}E$ of E onto $\mathcal{E}$, with respect to the energy inner product[6]. Then, in order to obtain (1) it is enough to put

$$E^e = P_{\mathcal{E}}E,\ E^a = E - P_{\mathcal{E}}E, T = \mathbb{C}P_{\mathcal{E}}E. \tag{2}$$

In the formulation currently implemented in MADY, there are three types of anelastic deformation, depending on the region of ∂E on which E is projected. They are the tensile, shear and compressive anelastic strains. An explicit expression of the stress has been determined when $\mathcal{E}$ is a polyhedron. Precisely, if $\mathcal{A}$ is a face of the polyhedron belonging to a plane having a normal M and a distance δ from the origin, it results

$$T = \mathbb{C}\left(E - \frac{(N \otimes M)E - \delta \mathrm{N}}{M \cdot N}\right), \tag{3}$$

where N is the outward unit normal to $\mathbb{C}\mathcal{A}$.

An elasto-plastic material is a material with memory, i.e., the stress at a material point depends on the history of all the deformations that took place at that point, but is independent of the strain rate. A (deformation) history is defined as a Lipschitz continuous mappings $E: [0,1] \rightarrow Sym$ (the space of all second order symmetric tensors), such that $E(0) = 0$. Moreover, it is assumed that there exists a constitutive functional that, for each history E and instant $\tau \in [0, 1]$, assigns the attained stress $T_E(\tau)$. The memory of elasto-plastic materials is characterized by the fact that, at every instant of each history, there exists a stress-free configuration that can be elastically reached from the current configuration. In addition, if damage is not taken into account, the elastic response of the material is not affected by previous plastic deformations.

Then, it is assumed that for each history E there is a plastic history E^p such that, for each $\tau \in [0, 1]$, the following conditions are satisfied: (i) the elastic strain $E^e = E - E^p$ belongs to the reduced elastic range $\mathcal{E}$; (ii) the stress reached at instant τ during history E depends linearly on E^e, i.e. $T_E = \mathbb{C}E^e$.

The stress range and the reduced elastic range may change during a history if the material

is allowed to undergo hardening or softening. Here, for the sake of simplicity, it is assumed that the material is ideally plastic and then $\mathcal{K}$ and $\mathcal{E}$ are fixed once and for all.

Let $E^e(\tau)\epsilon\,\partial\mathcal{E}$ be a regular point, and let $M(\tau)$ and $N(\tau)$ be the unit outward normals to $\partial\mathcal{E}$ at $E(\tau)$ and to $\partial\mathcal{K}$at $\mathbb{C}E^e(\tau)$, respectively. As usual the normality rule $\dot{E}^p = \left\|\dot{E}^p\right\|N$ is accepted and, moreover, $\partial\mathcal{E}$ is supposed to be locally defined by a smooth real function γ. Therefore, the following *flow rule* can be proved[9]

$$\left\|\dot{E}^p(\tau)\right\| = \begin{cases} 0, & \text{if } \gamma\left(E^e(\tau)\right) < 0, \\ 0, & \text{if } \gamma\left(E^e(\tau)\right) = 0 \text{ and } N(\tau)\cdot\dot{E}(\tau) \le 0, \\ \dfrac{M(\tau)\cdot\dot{E}(\tau)}{M(\tau)\cdot N(\tau)}, & \text{if } \gamma\left(E^e(\tau)\right) = 0 \text{ and } N(\tau)\cdot\dot{E}(\tau) > 0 \end{cases} \tag{4}$$

from which,

$$\dot{T} = \mathbb{C}\left(\mathbb{I} - \frac{(N\otimes M)}{M\cdot N}\right)\dot{E}, \tag{5}$$

with $\mathbb{I}$ the fourth order identity tensor, follows.

A comparison between the relationships (3) and (5) suggests that the normal elastic material is the Hencky 'version' of the elasto-plastic model. In other words, the two constitutive models correspond to the *deformation* and the *flow* theory of plasticity, respectively[9].

One of the main feature of the flow theory of plasticity is the "elastic unloading". For masonry, however, when a tensile anelastic strain - which represents the opening of fractures- is attained, it is not realistic to assume that a strain inversion induce compressive stress before that fractures are re-closed. Thus, the model proposed is elasto-plastic solely with reference to the compressive and shear behaviour, whereas it is nonlinear elastic in traction.

To better highlight the differences between the proposed plastic model and a fully (i.e. classical) elasto-plastic model, the results obtained for a simple case are provided in Fig. 1. The structure (see Fig. 1 a)) is a squat panel with 1.35 m height, having a rectangular cross-section 1 m in width and 0.25 m in thickness. It is perfectly clamped at its base with a further restrain to rotation at the top.

The main mechanical characteristics assumed are as follows: Young's modulus E = 1500 MPa, Poisson's ratio ν = 0.1, compressive strength σ_c = 3.0 MPa, tensile strength σ_t = 0, cohesion τ_0 = 0.3 MPa, friction parameter $\tan\varphi$ = 0.4 and density ρ = 1900 kg/m^3.

The panel has first been subjected to the vertical load q, which is equal to 0.6 MPa. Then, the cyclic process has been conducted by applying a vertical displacement at the top.

Fig. 1 b) shows the difference of the hysteresis curve obtained via the proposed model against the classical one.

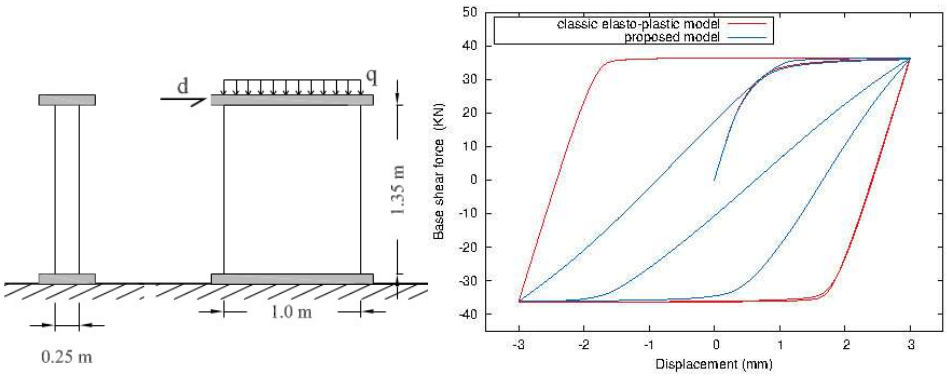

a) b)

Figure 1: a) sketch of the example case b) hysteresis curve of the proposed model, compared to that from the classical elasto-plastic model.

3 EXAMPLES OF APPLICATIONS

3.1 Static analysis of a groin vault

Some results from a static analysis of a groin vault are provided in the following. The analysed vault is a 4.92m*4.12m single span (within adjacent spans on both sides) of a vaulted cloister. It is set on the rear wall and on pillars in the side facing the cloister. The interaction with the remaining parts of the structure is accounted for via boundary conditions, while the infill has been considered as a dead load. The vault's thickness is 0.12m (except for the lateral arches whose thickness is 0.24m). Three chains are located on the lateral arches.

The structure is discretized by means of 800 thick shell elements, for 4125 degrees of freedom. Masonry is considered a non-linear elastic material with zero tensile strength. Values of the other mechanical parameters have been selected according to the Italian guidelines[14,15], accounting for the material safety factor γ_m = 3 and the Confidence Factor (CF) = 1.2 (for a building knowledge level LC2): Young's modulus E = 1.5 10^5N/cm^2, Poisson's coefficient $\nu = 0.1$, compressive strength σ_o = 89 N/cm^2; for bounded shear strength, cohesion τ_0 = 9 N/cm^2 and friction parameter tanφ = 0.4.

The mass density is assumed equal to 1.3*18 10^{-3} kg/cm^3 , while the infill density is 1.3*16 10^{-3} kg/cm^3; an uniform distributed load equal to 0.7 N/cm^2 has also been applied.

The numerical convergence has been achieved. Figs. 2 to 5 show some of the information provided by the code. Fig. 2 shows the mesh and the deformed configuration, while Fig. 3 gives a contour map of the compressive principal stress on the extrados of the vault. Fig. 4 and 5 depict the tensile and the shear anelastic strain, indicating the presence of fractures and sliding, respectively.

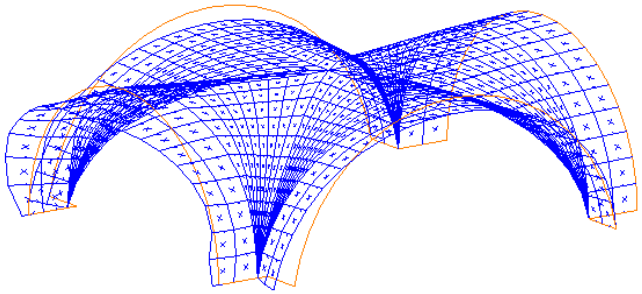

Figure 2: Mesh in the deformed configuration (amplified 100 times).

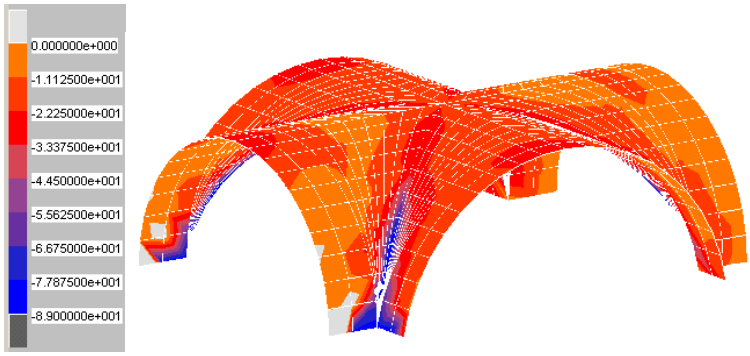

Figure 3: Compressive principal stress on the extrados of the vault.

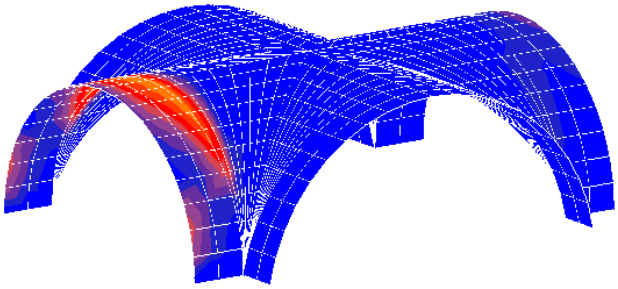

Figure 4: Tensile anelastic strain on the extrados of the vault.

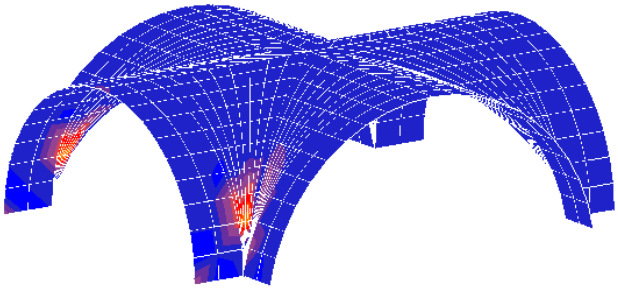

Figure 5: Shear anelastic strain on the extrados of the vault.

3.2 Dynamic analysis of a masonry tower

Results are provided for the structure proposed in literature[16] as an ideal scheme able to represent the main features of many existing Italian bell towers.

It's a free-standing tower, 27 m in height with a squared cross-section, 5.8 m in width; the geometry is extremely simplified, accounting solely for few typical elements: a door, a briefly and a change in wall's thickness from 1 to 0.85m occurring at the height of 11.5m.

Values of 3500 MPa, 3.5 MPa, 1900 kg/m^{3}and 0.1 have been adopted, respectively, for the Young's modulus E, the compressive strength σ_o, the mass density and the Poisson's coefficient ν. When a bounded shear strength is considered, the parameter of cohesion τ_0 has been assumed equal to 0.15 MPa, while the friction parameter $\tan\varphi$ is 0.4.

Dynamic (time-history) analyses has been conducted by applying, as earthquake input, the strong ground motion recorded during the Tabas, Iran event of 1978. The accelerogram has a magnitude of 7.4, a duration of 63.40s and a PGA of 0.925g. Moreover, a viscous damping coefficient of 4% for the first two flexural modes has always been used.

Fig. 6 shows the time-history of the displacement at the top of the tower, as obtained via a (3D) model - discretized through 810 shell elements, with a no-tension material behaviour and bounded compressive strength (referred in the following as NT model). The results obtained through a masonry-like beam model with an hollow rectangular cross-section are also shown to highlight the accuracy and type of information that such a model can provide. As can be seen, the two models experienced almost the same displacements at the top.

From a local perspective, the beam's predictions are also in good agreement with the 3D model predictions. At time t = 11.45s, where the first significant peak of the top displacement occurs, the two models provides the same values of the stress in the vertical direction and both highlight a zone, located near the tower's base, where crushing of the material occurs (Fig. 7 and 8). In terms of cracking, both the models predict a significant occurrence: the tower undergoes consistent tensile anelastic strain (see Fig. 7), emerging also in the beam model's from the amount of cracked areas (Fig. 8 b), c)). However, the location of cracking appears quite different. Although the (continuous) beam model can account for a distribution of cracking along the height of the tower (Fig. 8 c)), is not capable of giving the accurate description provided by the 3D model, which shows that cracking is much more extended in the upper part of the tower, with strong localization around the belfry.

A further comparison is presented accounting for a refinement of the constitutive law: a bound to shear stress is introduced in the 3D model, which is referred as BS model.

As shown by Fig. 9, differences in peak displacement are more pronounced, as shear strength is attained in the BS model. Fig 9 b) shows that the tensile anelastic strain (and the compressive anelastic strain as well) turn out to be similar to those obtained via the NT model, given in Fig. 7. However, as shown by Fig. 9 c), the tower undergoes a significant shear anelastic strain, with the consequent loss of stiffness and variation of amplitude and period in oscillation highlighted by Fig. 9 a). In the lateral view of the tower (depicted on the right in Fig. 9 c)), the effects of dilatancy can also be observed.

A further material's behaviour is considered, described by an elasto-plastic law, denoted as PL model. As shown by Fig. 10, where the response is compared with those of the NT and BS cases, it emerges that some variations has been obtained even with respect to the BS model, which has the same strengths domain but considers the material as normal elastic.

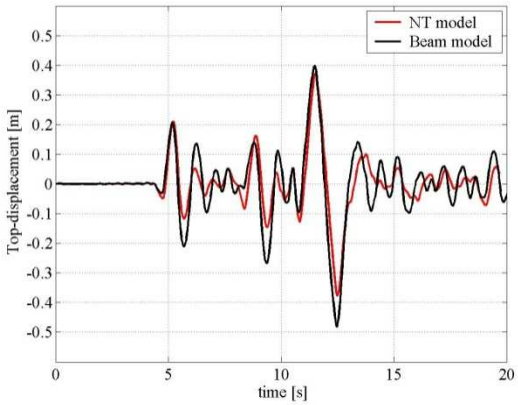

Figure 6. Time-history of the displacement at the top of the tower, obtained via the masonry-like 3D and the beam models.

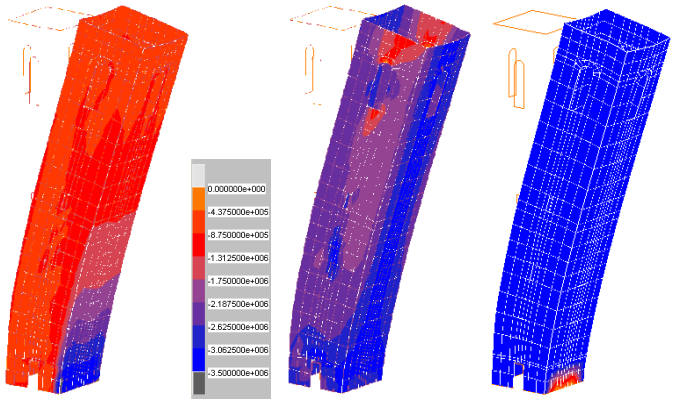

a) b) c)

Figure 7. 3D model results, at t = 11.45s: a) axial stress σ_z (Pa) in the vertical direction, anelastic strain due to b) traction and c) compression.

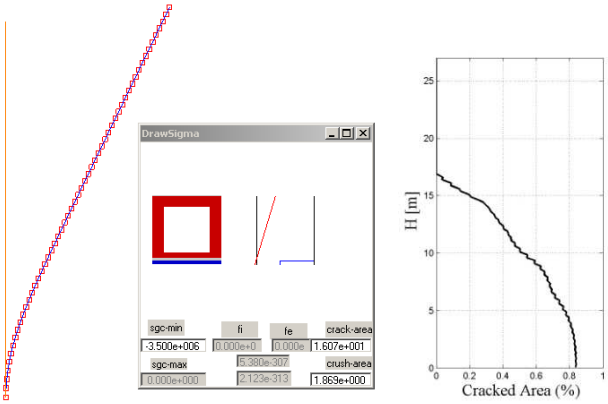

a) b) c)

Figure 8. Beam model results at t = 11.45s: a) deformed mesh, b) axial stress σ_z (Pa), cracking (red area) and crushing (blue area) at the tower's base; c) cracked area (% of the total area) along the height H of the tower.

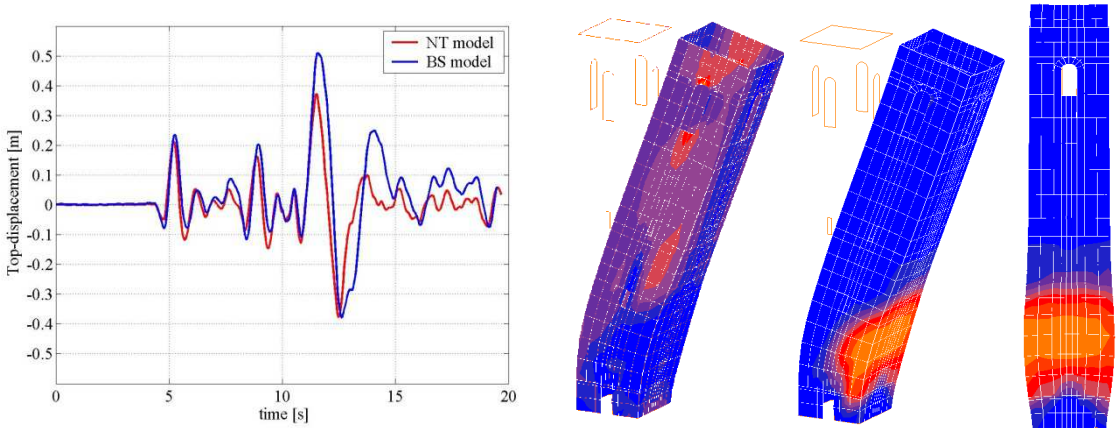

Figure 9. 3D model with bounded shear stress: a) time history, b) tensile anelastic strain and c) shear anelastic strain at t = 11.45s.

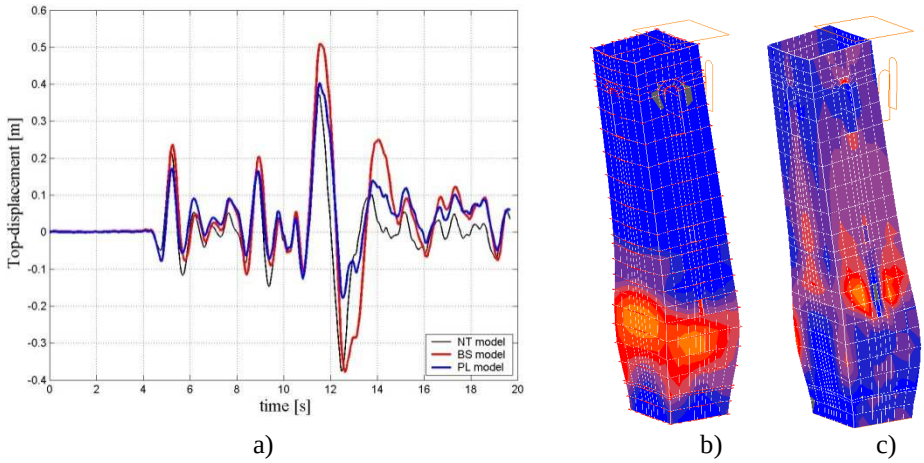

Figure 10. 3D plastic model: a) Time-history, b) plastic strain attained at t = 11.45s, c) overall tensile inelastic strain occurred until t = 11.45s.

3 CONCLUSIONS

The article presents the MADY computer code for the static and dynamic analysis of masonry buildings, which has been written by the authors for research purposes over the last ten years. While retaining its original features that make it easy to use and refined, the code now has a sufficient number of models to handle the analysis of many types of masonry structures. Of course, the class of materials can and should be further enriched.

The examples presented confirm the need for different types of models, both regarding the discretization of the structure in finite elements (beam, shell, 2D and 3D elements) and the constitutive characteristics of the material. In particular, despite the roughness of the beam element's formulation, it still allows for achieving a number of important indications. Moreover, the limit of shear strength, which is often neglected in studying masonry buildings, appears to be indispensable at least under certain load conditions.

REFERENCES

[1] M. Lucchesi and B. Pintucchi, "A numerical model for non-linear dynamics analysis of masonry slender structures", *Eur. J. Mech. A/Solids*, **26,** 88–105, (2007).

[2] B. Pintucchi and N. Zani, "Effects of material and geometric non-linearities on the collapse load of masonry arches", *Eur. J. Mech. A/Solids*, **28**, 45–61, (2009).

[3] B. Pintucchi, N. Zani, "Effectiveness of nonlinear static procedures for slender masonry towers", *Bull Earthquake Eng*, **12**, 2531–2556, (2014).

[4] M. Lucchesi, B. Pintucchi, M. Šilhavý and N. Zani, "On the dynamics of viscous masonry beams", *Cont. Mech. Thermodyn.*, 27, 349–365, (2015).

[5] M. Lucchesi, C. Padovani, G. Pasquinelli and N. Zani, *The constitutive equations of masonry-like materials*, Series: Lecture Notes in Applied and Computational Mechanics, Vol. 39, 19-50, Berlin Heidelberg, Springer-Verlag, (2008).

[6] M. Lucchesi, B. Pintucchi and N. Zani, "Bounded shear stress in masonry-like bodies", *Meccanica*, in press (2017).

[7] M. Lucchesi, C. Padovani, G. Pasquinelli and N. Zani, *Equilibrium of masonry bodies*, Series: Lecture Notes in Applied and Computational Mechanics, Vol. 39, 51-58, Berlin Heidelberg, Springer-Verlag, (2008).

[8] M. Lucchesi, C. Padovani, G. Pasquinelli and N. Zani, *The numerical method*, Series: Lecture Notes in Applied and Computational Mechanics, Vol. 39, 59-66, Berlin Heidelberg, Springer-Verlag, (2008).

[9] M. Lucchesi, B. Pintucchi and N. Zani, "A elasto-plastic model for masonry", AIMETA 2017 - XXIII Conference The Italian Association of Theoretical and Applied Mechanics, Salerno, Italy, 4–7 September 2017.

[10] B. Pintucchi and N. Zani, "A simple model for performing nonlinear static and dynamic analyses of unreinforced and FRP-strengthened masonry arches", *Eur. J. Mech. A/Solids*, **59**, 210–231, (2016).

[11] M. Lucchesi, B. Pintucchi and N. Zani, *Dynamic analysis of FRP-reinforced masonry arches via a no-tension model with damage*, Key Engineering Materials, (2015).

[12] G. Bartoli, M. Betti, P. Biagini, A. Borghini, A. Ciavattone, M. Girardi, G. Lancioni, A. Marra, B. Ortolani, B. Pintucchi, L. Salvatori, Epistemic Uncertainties in Structural Modeling: A Blind Benchmark for Seismic Assessment of Slender Masonry Towers, *J. Perform. Constr. Facil.*, 2017, 31(5): 04017067.

[13] M. Girardi, M. Lucchesi, C. Padovani, G. Pasquinelli, B. Pintucchi, N. Zani, *Numerical methods for slender masonry structures: A comparative study*, Proc. of the 11th International Conf. on Computational Structures Technology, B.H.V. Topping, (Editor), Civil-Comp Press.

[14] Ministero delle Infrastrutture e dei Trasporti (2008) Norme tecniche per le costruzioni—D.M. 14 Gennaio 2008. Supplemento Ordinario no. 30 Gazzetta Ufficiale no. 29 del 4-2-2008 (in Italian).

[15] Ministero delle Infrastrutture e dei Trasporti (2009) Istruzioni per l'applicazione delle "Nuove norme tecniche per le costruzioni". Circolare no. 617 del 2-2-2009 (in Italian).

[16] S. Casolo, V. Diana and G. Uva, "Influence of soil deformability on the seismic response of a masonry tower", *Bull Earthquake Eng*, **15**(5), 1991-2014, (2017).